Impact of Human Body Shape on Forced Convection Heat Transfer

Shri H. Viswanathan[1], Daniel M. Martinez[1], Lyle Bartels[1], Sai S. Guddanti[1], and Konrad Rykaczewski[1,2*]

1. School for Engineering of Matter, Transport and Energy, Arizona State University, Tempe, AZ 85287, USA
2. Julie Ann Wrigley Global Futures Laboratory, Arizona State University, Tempe, AZ 85287, USA

Address correspondence to:
Konrad Rykaczewski
School for Engineering of Matter, Transport and Energy
Arizona State University
Tempe, AZ 85287
*konradr@asu.edu

Orcid ID:
KR: 0000-0002-5801-7177

DECLARATIONS:

Funding: This research was supported by National Science Foundation Leading Engineering for America's Prosperity, Health, and Infrastructure (LEAP HI) #2152468 award (KR) and Master's Opportunity for Research in Engineering from Fulton Schools of Engineering at Arizona State University (SHV).

Acknowledgements: The authors also acknowledge Research Computing at ASU for providing High Performance Computing resources that have contributed to the research results reported within this paper.

Conflicts of interest/Competing interests: The authors declare no conflict of interest or competing interests.

Availability of data and material (data transparency): The manikin models will be made available on the ASU Dataverse website (dataverse.asu.edu) prior to publication.

Authors' contributions

Conceptualization: Methodology: KR, SHV, LB, DMM, SSG. Analysis: KR, SHV. Writing – Original Draft: SHV, KR. Writing – Review & Editing: SHV, KR, Final Review & Editing: SHV, KR, LB, DMM, SSG..

Word Count Main Manuscript: 4,000

Abstract

Predicting human thermal comfort and safety requires quantitative knowledge of the convective heat transfer between the body and its surrounding. So far, convective heat transfer coefficient correlations have been based only upon measurements or simulations of the average body shape of an adult. To address this knowledge gap, here we quantify the impact of adult human body shape on forced convection. To do this, we generated fifty three-dimensional human body meshes covering 1^{st} to 99^{th} percentile variation in height and body mass index (BMI) of the United States adult population. We developed a coupled turbulent flow and convective heat transfer simulation and benchmarked it in the 0.5 to 2.5 $m \cdot s^{-1}$ air speed range against prior literature. We computed the overall heat transfer coefficients, $h_{overall}$, for the manikins for representative airflow with 2 $m \cdot s^{-1}$ uniform speed and 5% turbulence intensity. We found that $h_{overall}$ varied only between 19.9 to 23.2 $W \cdot m^{-2} K^{-1}$. Within this small range, the height of the manikins had negligible impact while an increase in the BMI led to a nearly linear decrease of the $h_{overall}$. Evaluation of the local coefficients revealed that those also nearly linearly decreased with BMI, which correlated to an inversely proportional local area (i.e., cross-sectional dimension) increase. Since even the most considerable difference that exists between 1^{st} and 99^{th} percentile BMI manikins is less than 15% of $h_{overall}$ of the average manikin, it can be concluded that the impact of the human body shape on the convective heat transfer is minor.

Keywords. computational thermal manikin, forced convection simulation, turbulent flow, diverse human body shapes

List of Symbols, Abbreviations, & Constants

$h_{overall}$	Overall heat transfer coefficient, ($W \cdot m^{-2} K^{-1}$)
v	Air speed ($m \cdot s^{-1}$)
BMI	Body mass index ($kg \cdot m^{-2}$)

1.0 Introduction

Going to class early in the fall semester at Arizona State University is a walk through a convection oven. With air temperatures regularly soaring above 46°C (115°F), convective heating by the flowing hot air and the radiative heating from the sun and the concrete built-environment can rapidly lead to heat exhaustion. The Tempe campus alone has over 60,000 students and employees, so the experienced of "being cooked" along the walking path is shared by a large and diverse crowd. It is natural to wonder whether different individuals in this crowd are being "cooked" by the environment to the same degree. Excessive heat exposure can cause illnesses ranging from mild headaches to deadly heat strokes (Ebi et al. 2021b, a). Exposure to extreme heat is also becoming more prevalent, with estimates of about a third of the world population already experiencing it for at least 20 days a year (Mora et al. 2017). With continued unabated emissions of greenhouse gases, this fraction is predicted to increase to half or even three-quarters of the global population by the end of the century (Mora et al. 2017). Intriguingly, we currently do not know the degree to which the environment heats most individuals because our quantitative understanding of the process is restricted only to the "average" adult humans.

In extreme heat conditions, the human body is heated by the surrounding environment via radiation and convection and is cooled only through sweat evaporation (Parsons 2014). According to the Lewis analogy (Bergman et al. 2011), the rate of the latter cooling process is directly proportional to the convective heating rate (i.e., the mass transfer rate is proportional to the heat transfer rate). Accordingly, predicting the human thermal comfort and safety in extreme heat conditions requires a quantitative knowledge of the convective heat transfer coefficient for the human body. With relative air speeds above just a fraction of a meter per second, forced convection accounts for most of the heat transfer coefficient value (Fanger 1972).

The primary variable influencing the forced convection heat transfer coefficient (h_c) is the air velocity (v_a), with most of the available correlations taking the basic form of $h_c = cv_a^n$ originally proposed in 1939 by Winslow et al. (Winslow et al. 1939). The empirically determined coefficient c typically varies between 5 and 15, while the velocity exponent n is in the range of 0.4 to 0.6 (Wissler 2018; Xu et al. 2021a). Turbulence within the incoming air is also known to have a substantial impact on h_c, and its effects are accounted for by including turbulence intensity, and in a few cases length scale, in some modern correlations (Ono et al. 2008; Li and Ito 2012; Yu et al. 2020; Zou et al. 2020; Xu et al. 2021a; Zhou and Niu 2022). For human characteristics, correlations that account for the posture (e.g., standing, sitting, and laying down (Nishi and Gagge 1970; de Dear et al. 1997; Li and Ito 2012; Oliveira et al. 2014; Mao et al. 2017; Xu et al. 2019, 2021a)), the relative body orientation to the airflow direction (Xu et al. 2021a), and the effect of body motion (e.g., walking, running, cycling (Defraeye et al. 2011; Oliveira et al. 2014; Wissler 2018)) have been developed for the whole body and its parts.

As far as the human body shape, the available convective heat transfer correlations are based on measurements or simulations of manikins corresponding to neonatal babies (Sarman et al. 1992; Elabbassi et al. 2002; Belghazi et al. 2005; Ostrowski and Rojczyk 2018; Hannouch et al. 2020), 7-year-old child (Ito and Hotta 2006), and, in the vast majority, the average female or male adult (e.g., the 50th percentile body mass index (BMI) and posture for the Western population (Dreyfuss and Dreyfuss 1967; Fromuth and Parkinson 2008)). However, most of us are not "average" and what an "average" body shape is varies across regions and cultures (Lin et al. 2004; Daniell et al. 2012; Davoudiantalab et al. 2013). As evident from **Fig.1** which shows body shape diversity for the adult population of the United States, substantial geometrical differences from the "average" are common. In this work, we build on our recent research on the impact of body shape on radiative heat transfer (Rykaczewski et al. 2022a, c) and use computational means to quantify how the body shapes in our diverse population impact the forced convection heat transfer coefficient.

2.0 Methods

2.1 Generation of three-dimensional human body models

To conduct the flow simulations, we smoothened the human body meshes which we previously generated to study radiative area factors (Rykaczewski et al. 2022b, a). We extracted the original three-dimensional human body models from the Open Design Lab Manikin Fetcher tool based on US National Health and Nutrition Examination Survey (NHANES) (Parkinsons). This database covers 1st to 99th percentile variation in height and BMI of the United States adult population. We exported twenty-five manikins for each gender covering each height and BMI percentile combination in about 25% increments. The manikin shapes that we processed account for tight-fitting shorts and T-shirts (these result in only exterior simplification, see Supplemental Information), but had scalp hair and hands removed. All manikins are in a standing pose with arms raised at 35° away from the trunk. Previously, we cleaned these fifty human body meshes to remove all non-manifold edges and vertices and uploaded the results as .stl files to the Physical and Computational Thermal Manikins Database (Rykaczewski et al. 2022b). To facilitate the convergence of the flow simulations, we used the Autodesk Meshmixer software to smooth locally uneven surfaces, especially along the inner thighs, the armpits, and the feet. We carried out these local smoothing operations using Robust Smooth, Adaptive Reduce, and Refine tools in the software. We note that the smoothening process had a negligible effect on the original human body shape (e.g., the processing caused less than 1% of the total surface area of the manikins to change). The smoothened manikins were imported as .stl files into COMSOL Multiphysics 6.0 software, where after several additional steps discussed next "watertight" meshes representing volume around the manikins were created.

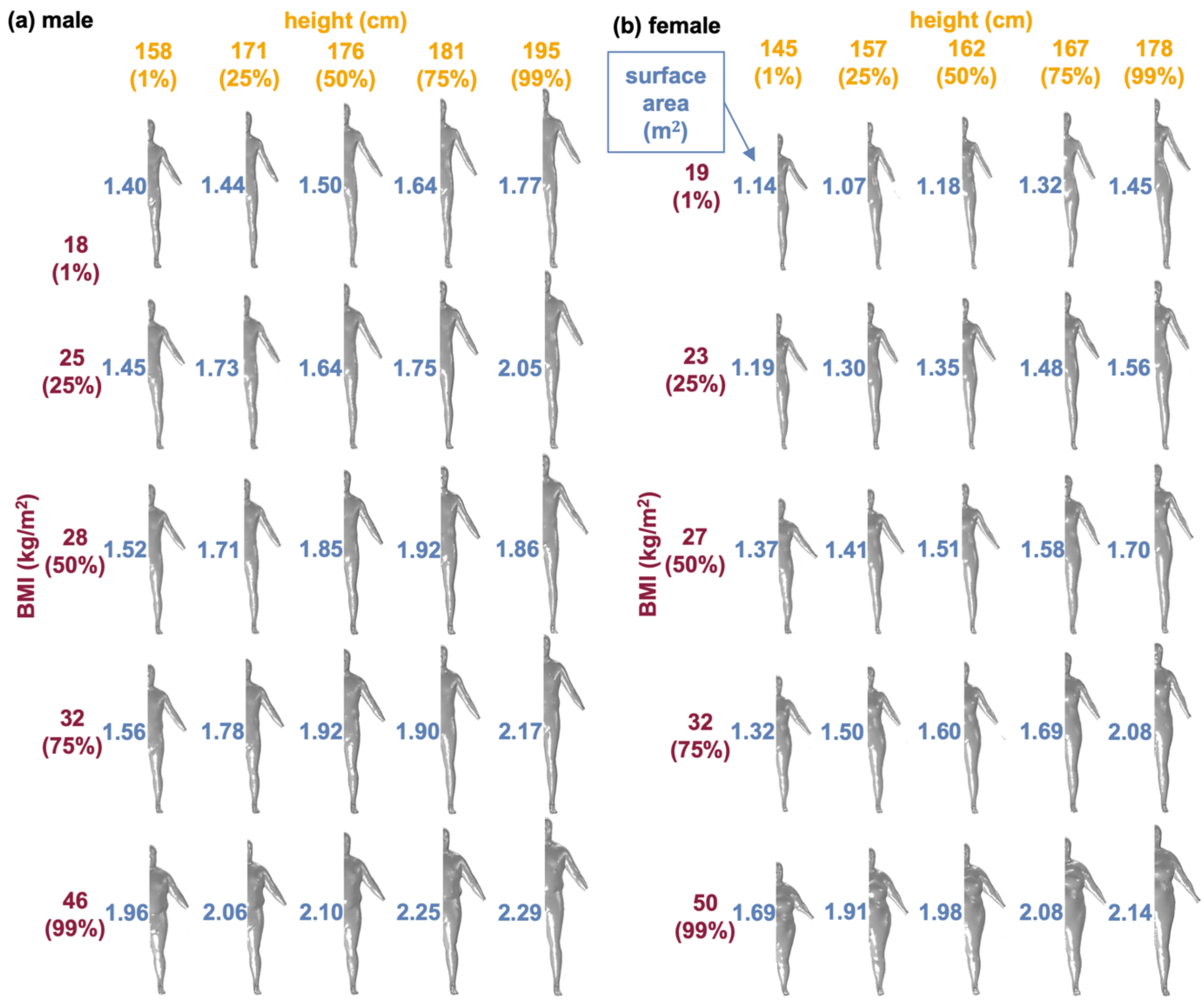

Fig.1 The smoothed twenty-five (a) male and (b) female half-manikin shapes presented as a function of the height and BMI values and corresponding population percentiles along with the total body surface areas (A_t for the full manikin).

2.2 Flow and forced convection simulation formulation

We simulated coupled turbulent flow and convective heat transfer from the manikins using the finite element method implemented in Comsol Multiphysics 6.0. Our formulation follows the experimentally validated Xu et al.(Xu et al. 2019, 2021a, b) methodology including the numerical solution of the steady-state Reynolds Averaged Navier Stokes using the weakly compressible Low Reynolds number k-ε model and the constant manikin surface temperature boundary condition. In particular, following Xu et al. (Xu et al. 2019, 2021a, b) and typical conditions specified by physical manikin operating standards (Parsons 2014), we set the surface temperature to 35ºC and the air temperature to 25ºC. In reality, the temperature can vary by even 5ºC across different body parts (Fournet et al. 2013; Coull et al. 2021). However, as even large difference in the air temperature and pressure, the skin temperature variation will have negligible to minor impact on the heat transfer coefficient value (but will impact the convective heat gain or loss that is proportional to skin-to-air temperature difference—see discussion in Supplemental Information).

The manikins are located in the center of an elongated flow chamber and face the airflow. At the inlet, the uniform air flow has a turbulence intensity of 5%, typical for human heat transfer coefficient measurements (Xu et al. 2021a), and a turbulence length scale of 5 cm (comparable to the default 7% of the inlet geometrical length scale used by Xu et al.(Xu et al. 2019, 2021a, b)). We computed the h_{overall} by diving the average heat flux for the entire body surface area output by the Comsol Multiphysics software ("Derived Average Value" of the "ht.ntflux" variable) by the skin-to-air temperature difference of 10ºC. We note that natural convection has a negligible contribution to the overall heat transfer coefficient at velocities above 0.5 $m \cdot s^{-1}$ (Xu et al. 2019). For example, in the case of our average male manikin exposed to 0.5 $m \cdot s^{-1}$ air flow with a 10ºC surface-to-air temperature difference, including free convection increased h_{overall} only by ~0.2 $W \cdot m^{-2} K^{-1}$ or 2%. Since the impact of natural convection for higher velocities is even further diminished, we did not simulate buoyancy effects in the rest of the simulations. We will address the topic in a separate dedicated study.

To reduce the computational time, we applied symmetry conditions on the sagittal plane of the manikins (see **Fig.2a**). We note that the leg posture in our manikins is slightly asymmetric. However, there is less than 1% left-to-right side difference in the overall heat transfer coefficient (h_{overall}). Since simulating hands requires a dense mesh and the corresponding local heat transfer coefficient is highly dependent on hand orientation (Zhang et al. 2021b, a), we removed them from the manikins with a straight cut across the wrist. To generate a higher density mesh near the manikin, we discretized the 4 m long, 2.5 m wide, and 2.4 m tall flow chamber into two regions. We adjusted the internal region size to each manikin so that the boundaries of the inner part were separated from the human shape at least by 0.15 to 0.25 m (the latter also being the floor-to-foot height). Increasing the size of the inner or outer region had negligible effects on the heat transfer coefficient. To generate the mesh, we specified the triangular element distribution on the manikin surface and then generated the tetrahedral and the boundary layer elements (using the default setting of 8 layers with 1.2 stretching factor) within the inner and later the outer regions. We adjusted the total boundary layer thickness near the manikin surface to the geometry and air velocity so that the "distance to cell center in viscous units" was below or near the 0.5 value recommended by Comsol Multiphysics. After conducting mesh refinement studies (see example in **Fig.2b**), we utilized triangular elements with a maximum of 2.5 cm size, matching Xu et al. (Xu et al. 2021a) and a specified minimal size of 1 cm (further increasing the mesh density by 50% only increased heat transfer coefficient by 0.5%). We found that the latter avoided meshing issues on the more complex manikin surfaces. The maximum and minimum tetrahedral element sizes in the inner regions were 6.4 and 0.75 cm and 11.6 cm and 3.46 cm in the outer region. We note that to achieve the minimum element quality ("skewness") near 0.1, we adjusted the "element quality optimization" setting for the two tetrahedral mesh segments between "basic" and "medium" (counterintuitively the "basic" setting sometimes yielded higher quality mesh).

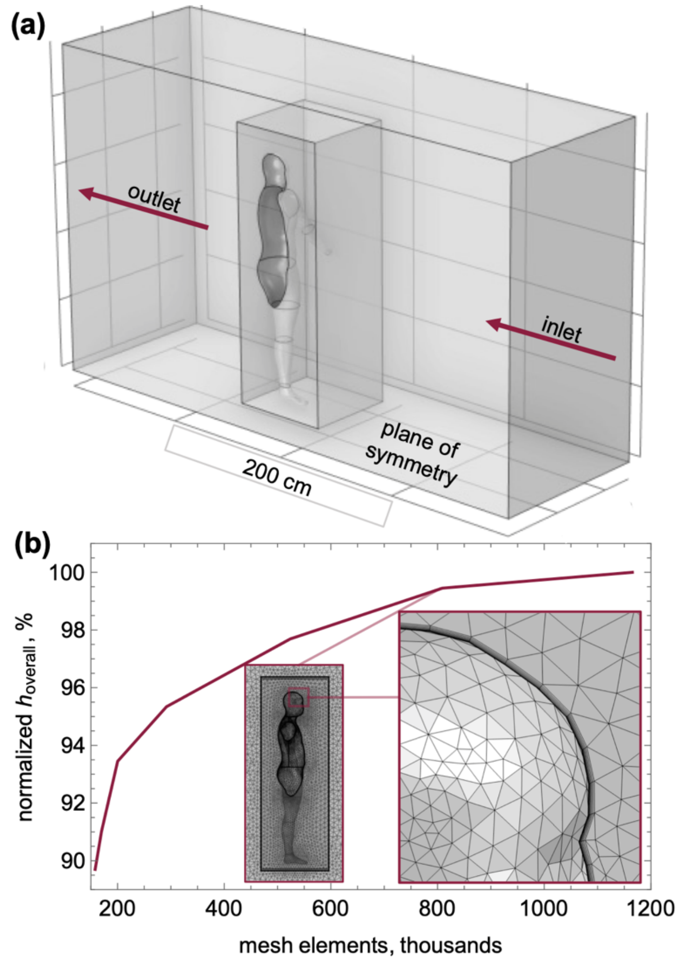

Fig.2. (a) schematic of the simulated flow chamber and (b) example mesh refinement study presented in normalized units to facilitate interpretation.

3.0 Results

3.1 Overall convective heat transfer coefficient for the average (western) male

Before quantifying body shape variation's impact on heat transfer coefficient, we first benchmark our convection simulations for the average (western) male manikin against the Xu et al. simulation-based correlation (see Table S1 in Supplemental Information (Xu et al. 2019, 2021a, b)). The Xu et al. model on which we based our simulation formulation was validated against matching thermal manikin measurements (Xu et al. 2019). To match their computational manikin pose, we simulate a manikin with arms along the trunk in addition to the same manikin but with arms oriented away from the body (i.e., the output pose from the manikin fetcher tool

(Parkinsons)). We simulate the $h_{overall}$ for incoming air velocity of 0.5 to 2.5 $m\cdot s^{-1}$ that Xu et al. simulated (Xu et al. 2019, 2021a, b). This range also covers over 90% of conditions in our recent outdoor measurements during 58 warm-to-hot days in Tempe, Arizona (Vanos et al. 2021).

The plot in **Fig.3** shows that the manikin arm position has a negligible impact on the $h_{overall}$ and that our results match closely with Xu et al.(Xu et al. 2021a). Specifically, below 1.5 $m\cdot s^{-1}$ our results overlap with those Xu et al.(Xu et al. 2021a). The 1 to 2 $W\cdot m^{-2}K^{-1}$ discrepancy between our results and those of Xu et al.(Xu et al. 2021a) in the 1.5 to 2.5 $m\cdot s^{-1}$ range might stem from geometrical differences between our manikins (i.e., average western—176 cm and 1.89 m^2 vs. average Asian—172 cm and area of 1.65 m^2 males (Xu et al. 2019)—see geometry overlay in the Supplemental Information) and their positions in the flow chambers. It is worth keeping in mind when comparing minor differences in convective heat transfer coefficients that the experimental uncertainty is often in the 2 to 2.5 $W\cdot m^{-2}K^{-1}$ range (95% confidence interval). Considering such uncertainty, our results would statistically overlap with Xu et al.(Xu et al. 2021a). We note that there are numerous other correlations for $h_{overall}$ that are based on a variety of simulation and measurement approaches that provide substantially different predictions (see Supplemental Information). The reasons for this large $h_{overall}$ scatter in the literature has not yet been rooted out and is beyond the scope of current work. Irrespective, the close match between our $h_{overall}$ simulations and Xu et al. results on which we based our formulation provides sufficient validation of our model for evaluating the relative impact of human body shape on the convective process.

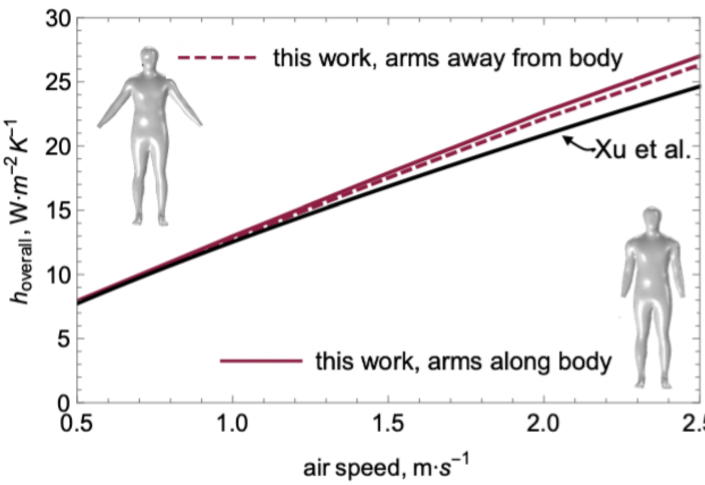

Fig.3. The overall convective heat transfer coefficient, h_{overall}, for the average adult (western male in our simulations not accounting for hands) as a function of air speed, comparing our results for male manikin with arms along and away from the body against Xu et al. 2021 results on which we based on model formulation. For our simulations, the turbulence intensity was set to 5% and the turbulence length scale was set to 5 cm.

3.2 Overall convective heat transfer coefficients for diverse body shapes

We simulated h_{overall} for the twenty-five male and twenty-five female manikins exposed to 2 $m\cdot s^{-1}$ uniform airflow with a turbulence intensity of 5% and a turbulence length scale of 5 cm. The values summarized in **Table 2** demonstrate that despite the relatively large shape and surface area differences (see Fig.1), all values are within 19.9 to 23.2 $W\cdot m^{-2}K^{-1}$ range. The h_{overall} for the average (50th percentile BMI and height) male and female manikins are nearly identical at 22.1 and 22.2 $W\cdot m^{-2}K^{-1}$, respectively. The largest h_{overall} variations from these average values are −8.1% for the 99% BMI and 99% height male manikin and −8.1% for the 99% BMI and 75% height female manikin. Several consistent trends emerge within this relatively minor variation, which we discuss next.

Table 2. Impact of body shape on the overall forced convection heat transfer coefficients ($W\cdot m^{-2}K^{-1}$) for uniform inlet velocity of 2 $m\cdot s^{-1}$ with a turbulence intensity of 5% and a turbulence length scale of 5 cm.

male manikins							**female manikins**					
	BMI, percentile							**BMI, percentile**				
height, percentile	**1**	**25**	**50**	**75**	**99**		**height, percentile**	**1**	**25**	**50**	**75**	**99**
1	22.7	22.3	22.5	21.8	20.4		**1**	23.1	22.9	22.1	22.1	20.4
25	22.9	22.4	22.1	21.8	20.3		**25**	23.2	22.8	22.3	21.8	20.7
50	22.8	22.5	22.1	21.8	20.3		**50**	23.2	22.6	22.2	21.4	20.3
75	22.6	22.3	21.8	21.6	20.4		**75**	23.2	22.5	22.3	21.8	19.9
99	22.3	22.2	21.8	21.5	20.3		**99**	22.4	21.9	22.4	21.8	20.1

To facilitate observation of how body shape impacts the heat transfer coefficient, in **Fig.4** we plotted example variations in $h_{overall}$ for manikins with either fixed height (at 1%, 50% and 99%) and varied BMI, or fixed BMI (at 1%, 50% and 99%) with varied height. The results are plotted in population percentile terms in **Fig.4a&c** and absolute height or BMI terms in **Fig.4b&d**. The most pronounced decrease in $h_{overall}$ occurs with increasing BMI. In particular, the $h_{overall}$ decreases nearly linearly with BMI at a rate of 0.07 to 0.09 $W{\cdot}m^{-2}K^{-1}$ per $kg{\cdot}m^{-2}$ for both the male and the female manikins. In absolute terms, over the entire range of the BMI, the $h_{overall}$ varies by 2.3 to 3.3 $W{\cdot}m^{-2}K^{-1}$. In contrast, the variation in height of the manikins has a much smaller impact on the $h_{overall}$. In particular, the $h_{overall}$ decreases only by 0.1 to 1 $W{\cdot}m^{-2}K^{-1}$ over the entire height range. Next, we discuss whether any body segment provides a dominant contribution to the BMI impact on the $h_{overall}$.

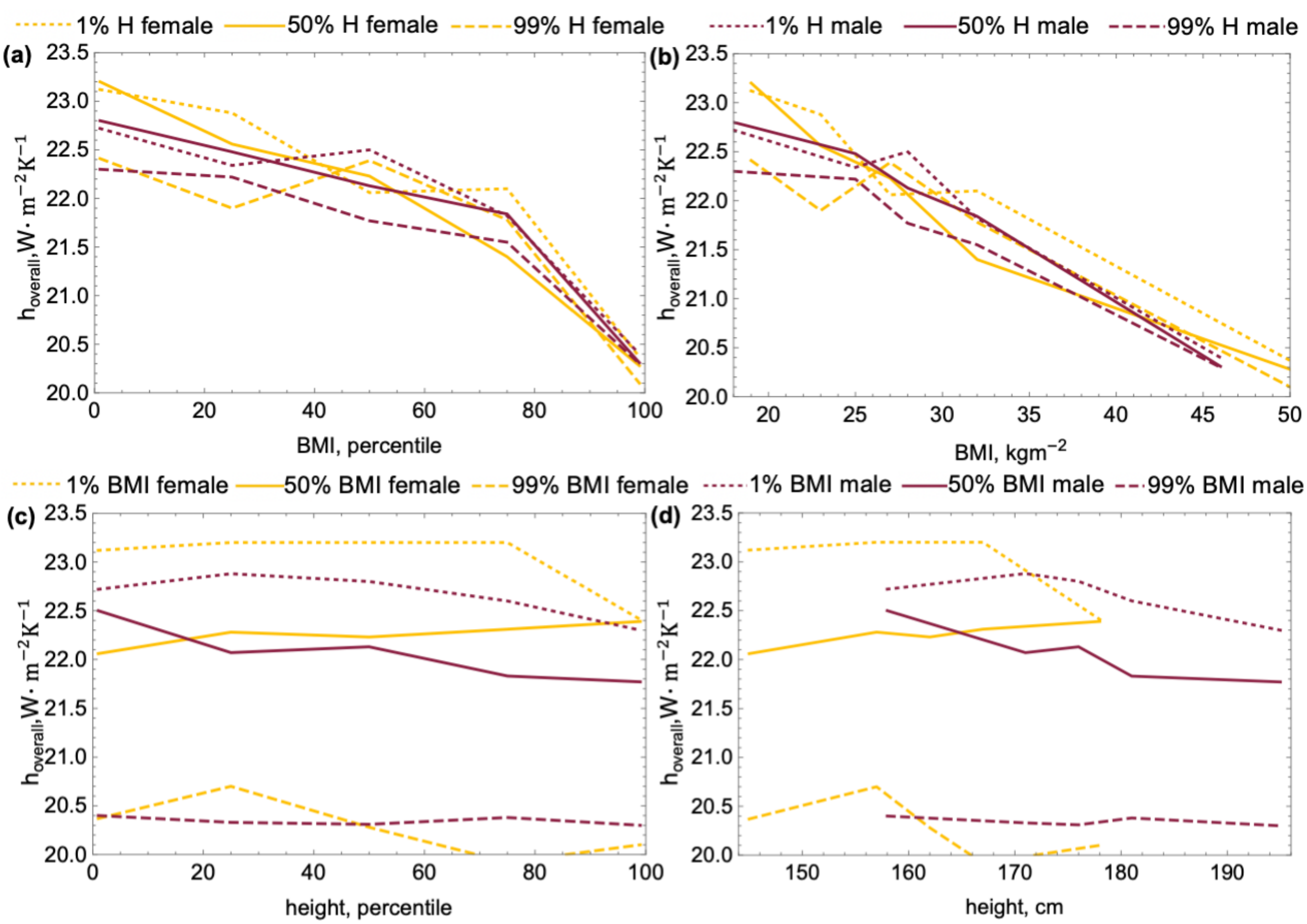

Fig.4. Example variation in the $h_{overall}$ for manikins with either fixed height (at 1%, 50%, and 99%) with varied BMI in (a) population percentile and (b) absolute terms, and manikins with BMI fixed (at 1%, 50%, and 99%)

with varied height in (c) population percentile and (d) in the absolute terms. The simulation settings include inlet air speed of 2 m·s^{-1}, turbulence intensity of 5%, and turbulence length scale of 5 cm.

4. Discussion

Fig. 5a shows the heat transfer coefficient distribution for the front and the back of the average height male manikins with 1%, 50%, and 99% BMI. To facilitate quantitative comparison, the bar plot in **Fig. 5b** shows the overall and local heat transfer coefficients for the manikin zones shown in the inset in **Fig. 5c**, along with equivalent results from Xu et al.(Xu et al. 2021a) for the computational manikin based on scanned Newton_asia instrument. The latter agree within ~1 W·m^{-2}K^{-1} with our "average guy" results and diverge at most by 3 to 3.5 W·m^{-2}K^{-1} for the head and back areas. These differences likely stem from the disparity between the two manikins' shoulder (trapezius muscle whose posterior part is included in the back segment) and neck regions (included in the head segment) that are evident in the manikin silhouettes (see inset in **Fig.5c** and the Supplemental Information).

Regarding the definition of the body regions, we note that for the 1% and 99% BMI manikins, we computed values for the upper leg and pelvic areas in two ways. The reason for introducing these two definitions is that our manikins are "wearing" tight-fitting shorts and T-shirt (Parkinsons; Rykaczewski et al. 2022c), which translates into a slightly merged crotch area (i.e., the larger manikin appears to have shorter legs due to overlap of the upper thighs that are blended by the shorts). Accordingly, in the first definition of the upper leg and pelvic area borders is at the height of the crotch of the individual manikins. In the second definition, the upper leg and pelvic area boundary is at the height of the 50% BMI manikin's border for all manikins. We found that the difference between the local heat transfer coefficients calculated using the two region definitions were only around 0.1 W·m^{-2}K^{-1}, so we report all the values using the more consistent second definition.

Except for unaffected values for the head, the lower leg, and the foot, the local heat transfer coefficients generally decrease with increasing BMI of the manikins. By also evaluating **Fig. 5c**, we see that the decrease in the local heat transfer coefficients correlates with the increase of the body segment area with increasing BMI.

Physically, this trend stems from the reduction of the heat transfer coefficient induced by the rise of the cross-sectional dimensions of the body segments indicated by the surface area increase. Since the individual body parts are often approximated as cylinders (Fiala et al. 1999; Fiala and Havenith 2015), we can evaluate this trend by referring to the pertinent heat transfer correlations. In particular, in the relevant 4,000 to 40,000 Reynold's number range, both the Hilpert (Hilpert 1933) and Zukauskas (Bergman et al. 2011) correlations indicate that the average heat transfer coefficient scales with $D^{-0.4}$. In other words, for a relatively small diameter, D, increase with a decrease in BMI, we can expect an approximately proportional linear reduction in the corresponding heat transfer coefficient.

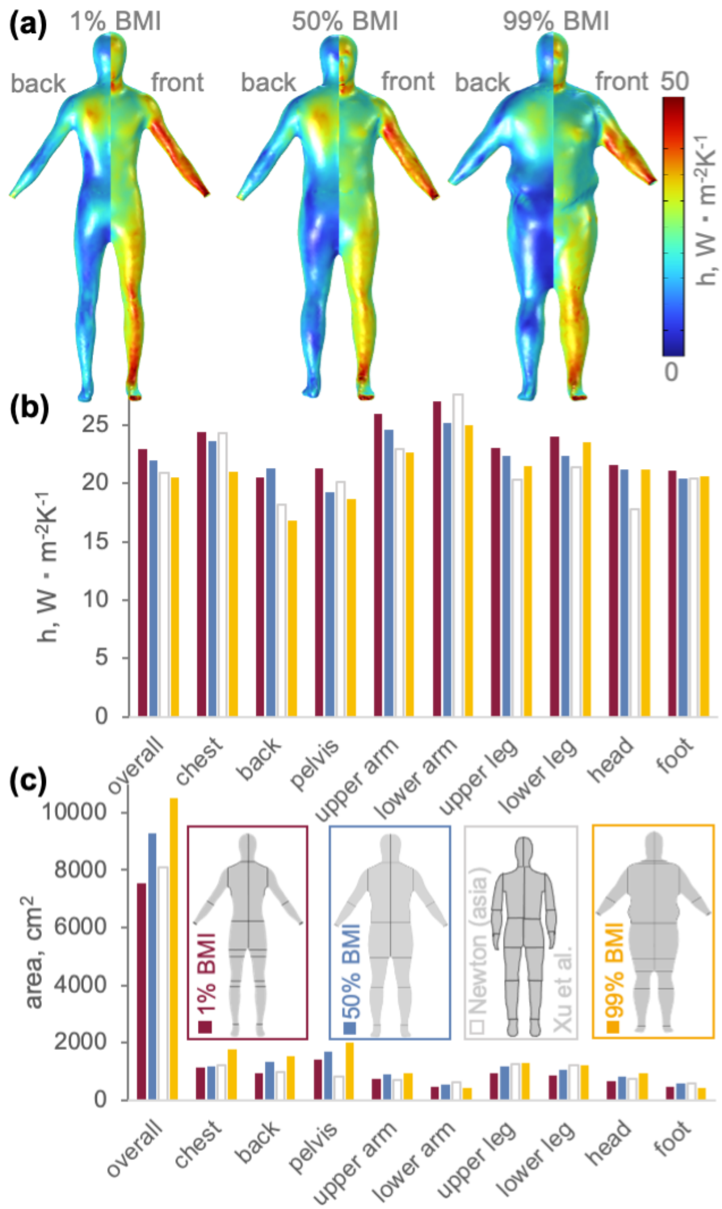

Fig.5. (a) The heat transfer coefficient (h) distribution on the front and back of the manikins, and the overall (excluding hand) and local **(b)** convective heat transfer coefficients, and **(c)** areas for indicated body regions for the 50% height male manikins with 1%, 50%, and 99% BMI along with equivalent results from Xu et al.(Xu et al. 2021a) for the Newton_asia computational manikin (areas are based on summation of segments of the physical instrument provided by the instrument manufacturer). The simulation settings include an inlet air speed of $2\ m\cdot s^{-1}$, turbulence intensity of 5%, and turbulence length scale of 5 cm.

It is worth pointing out that since the $\mathrm{h}_{\mathrm{overall}}$ decrease with increasing BMI is relatively small, the overall convective heat gain rate ($A_t \mathrm{h}_{\mathrm{overall}} \Delta T_{skin-air}$) increases with height and with most BMI values. For the latter, the heat gain rate increase is substantial from 1 to 75% BMI (see Supplemental Information). When BMI increases from 75% to 99%, the $\mathrm{h}_{\mathrm{overall}}$ decreases most rapidly, which leads to either minor increase or decrease of the overall heat gain rate. For example, for a 12°C skin-to-air temperature difference ($\Delta T_{skin-air}$) that a typical person would experience while walking in 46°C during summer in Tempe, AZ (assuming a mean skin temperature of 34°C (Haslam and Parsons 1987; Parsons 2019; Coull et al. 2021)), a 50% height and 1% BMI male convectively gains 415.9 W while a 50% height and 75% male gains 503.2 W. However, in the same conditions a 50% height and 99% BMI male gains 453.3 W (see Supplemental Information for more details). It is important to keep in mind that a higher convective heat gain does not necessarily translate to a proportionally higher body core temperature for multitude of factors. For example, a higher convective heat gain will be linked to a higher sweat evaporation rate and a higher BMI to a larger body mass (i.e., higher heat storage capacity). To quantify impact on the core temperature evolution, all factors contributing to the human heat balance must be evaluated (Parsons 2014).

5. Conclusions

In summary, we computationally investigated the impact of adult human body shape on forced convective heat transfer. In particular, we created fifty computational manikins that represent the 1% to 99% BMI and height diversity of the United States population. We formulated a coupled turbulent flow and convective heat transfer simulation and benchmarked it against available literature. At the representative conditions of 2 $\mathrm{m \cdot s^{-1}}$ uniform airflow with a turbulence intensity of 5% and length scale of 5 cm, our results demonstrate that the $h_{overall}$ for all manikins are within 19.9 to 23.2 $\mathrm{W \cdot m^{-2} K^{-1}}$ range. The largest variations of $h_{overall}$ from the 22.1 to 22.2 $\mathrm{W \cdot m^{-2} K^{-1}}$ values for the average shapes are −8.1% for the male the 99% BMI and 99% height male manikin and −8.1% for the 99% BMI and 75% height female manikin.

Within this relatively minor variation, we found that height has a negligible impact on convective heat transfer, while the increase in BMI correlates to a proportional decrease in the $h_{overall}$. In particular, the $h_{overall}$ decreases nearly linearly with BMI at a rate of 0.07 to 0.09 $W \cdot m^{-2}K^{-1}$ per kgm^{-2} which translates to 2.3 to 3.3 $W \cdot m^{-2}K^{-1}$ variation over the entire BMI range. Except for unaffected values for the head, the lower leg, and the foot, we found that the local heat transfer coefficients generally decrease with increasing BMI, and with that increasing local area and cross-sectional dimension of the manikins. This trend agrees with classical correlations for cylinders in cross-flow, for which the heat transfer coefficient scales as $D^{-0.4}$. Consequently, the primary reason for decreasing the heat transfer coefficients with increasing BMI is the corresponding increase in the equivalent cross-sectional dimensions of the body components. However, we emphasize that even the largest $h_{overall}$ variation that occurs between the 1 and 99% BMI manikins is minor (i.e., below 15% of $h_{overall}$ for the average manikin). Since we reached similar conclusions regarding body shape impact on the radiative area factors (Rykaczewski et al. 2022a), the human body surface area provides an excellent scaling factor for human-surrounding radiative and convective heat transfer processes. Thus, the human body shape should not significantly impact the thermal comfort and safety calculations based on the classical body heat balance equation (Fanger 1972).

REFERENCES

Belghazi K, Elabbassi EB, Tourneux P, Libert J (2005) Assessment of whole body and regional evaporative heat loss coefficients in very premature infants using a thermal mannequin: influence of air velocity. Med Phys 32:752–758

Bergman TL, Lavine AS, Incropera FP, Dewitt DP (2011) Fundamentals of heat and mass transfer. John Wiley & Sons, Inc, New York

Coull NA, West AM, Hodder SG, et al (2021) Body mapping of regional sweat distribution in young and older males. Eur J Appl Physiol 121:109–125

Daniell N, Fraysse F, Paul G (2012) How does the size and shape of local populations in China compare to general anthropometric surveys currently used for product design? Work 41:4088–4090

Davoudiantalab AHDA, Meshkani M, Nourian S, Mofidi AA (2013) Anthropometric dimensions of Iranian male workers and comparison with three Asian countries. International Journal of Occupational Hygiene 5:166–171 de Dear RJ, Arens E, Hui Z, Oguro M (1997) Convective and radiative heat transfer coefficients for individual human body segments. Int J Biometeorol 40:141–156

Defraeye T, Blocken B, Koninckx E, et al (2011) Computational fluid dynamics analysis of drag and convective heat transfer of individual body segments for different cyclist positions. J Biomech 44:1695–1701

Dreyfuss H, Dreyfuss H (1967) The measure of man: human factors in design. Whitney Library of Design New York

Ebi KL, Capon A, Berry P, et al (2021a) Hot weather and heat extremes: health risks. The Lancet 398:698–708

Ebi KL, Vanos J, Baldwin JW, et al (2021b) Extreme weather and climate change: population health and health system implications. Annu Rev Public Health 42:293

Elabbassi EB, Chardon K, Bach V, et al (2002) Head insulation and heat loss in naked and clothed newborns using a thermal mannequin. Med Phys 29:1090–1096

Fanger PO (1972) Thermal Comfort. McGraw-Hill Book Company, New York

Fiala D, Havenith G (2015) Modelling human heat transfer and temperature regulation. In: The mechanobiology and mechanophysiology of military-related injuries. Springer, pp 265–302

Fiala D, Lomas KJ, Stohrer M (1999) A computer model of human thermoregulation for a wide range of environmental conditions: the passive system. J Appl Physiol

Fournet D, Ross L, Voelcker T, et al (2013) Body mapping of thermoregulatory and perceptual responses of males and females running in the cold. J Therm Biol 38:339–344

Fromuth RC, Parkinson MB (2008) Predicting 5th and 95th percentile anthropometric segment lengths from population stature. In: International Design Engineering Technical Conferences and Computers and Information in Engineering Conference. pp 581–588

Hannouch A, Habchi C, Lemenand T, Khoury K (2020) Numerical evaluation of the convective and radiative heat transfer coefficients for preterm neonate body segments inside an incubator. Build Environ 183:107085

Haslam RA, Parsons KC (1987) A comparison of models for predicting human response to hot and cold environments. Ergonomics 30:1599–1614

Hilpert R (1933) Heat transfer from cylinders. Forsch Geb Ingenieurwes 4:215

Ichihara M (1997) Measurement of Convective and Radiative Hear Transfer Coefficients for the Standing and Sitting Human Body Using a Thermal Manikin. J Archit Plann Environ Eng, AIJ 501:45–51

Ito K, Hotta T (2006) Development of Virtual Manikins and its grid library for CFD Analysis. 空気調和・衛生工学会論文集 27–33

Li C, Ito K (2012) Numerical analysis of convective heat and mass transfer around human body under strong wind. International Journal of High-Rise Buildings 1:107–116

Lin Y-C, Wang M-JJ, Wang EM (2004) The comparisons of anthropometric characteristics among four peoples in East Asia. Appl Ergon 35:173–178

Mao N, Song M, Pan D, Deng S (2017) Computational fluid dynamics analysis of convective heat transfer coefficients for a sleeping human body. Appl Therm Eng 117:385–396

Martinho N, Lopes A, Silva MCG, et al (2007) Human Numerical Model for Evaluation of Thermal Comfort in Vehicles. In: 1th European Automotive Congress - Automobile for the Futur. Budepest, pp 1–10

Mora C, Dousset B, Caldwell IR, et al (2017) Global risk of deadly heat. Nat Clim Chang 7:501–506

Nishi Y, Gagge AP (1970) Direct evaluation of convective heat transfer coefficient by naphthalene sublimation. J Appl Physiol 29:830–838

Oguro M, Arens E, ZHANG H, KATAYAMA T (2002) Convective heat transfer coefficients and clothing insulations for parts of the clothed human body under airflow conditions. Journal of Architecture and Planning (Transactions of AIJ) 67:21–29

Oliveira AVM, Gaspar AR, Francisco SC, Quintela DA (2014) Analysis of natural and forced convection heat losses from a thermal manikin: Comparative assessment of the static and dynamic postures. Journal of wind engineering and industrial aerodynamics 132:66–76

Ono T, Murakami S, Ooka R, Omori T (2008) Numerical and experimental study on convective heat transfer of the human body in the outdoor environment. Journal of Wind Engineering and Industrial Aerodynamics 96:1719–1732

Ostrowski Z, Rojczyk M (2018) Natural convection heat transfer coefficient for newborn baby. Heat and Mass Transfer 54:2395–2403

Parkinsons M Open Design Lab Manikin Fether. http://tools.openlab.psu.edu/tools/fetcher.php

Parsons K (2014) Human thermal environments: the effects of hot, moderate, and cold environments on human health, comfort, and performance. CRC press

Parsons K (2019) Human heat stress. CRC Press

Rykaczewski K, Bartels L, Martinez DM, Viswanathan SH (2022a) Human body radiation area factors for diverse adult population. Int J Biometeorol 66:2357–2367

Rykaczewski K, Bartels L, Martinez DM, Viswanathan SH (2022b) Computational manikin for radiation simulation (male and female models covering 1-99% BMI and height diversity in US. https://dataverse.asu.edu

Rykaczewski K, Vanos JK, Middel A (2022c) Anisotropic radiation source models for computational thermal manikin simulations based on common radiation field measurements. Build Environ 208:108636

Sarman I, Bolin D, Holmér I, Tunell R (1992) Assessment of thermal conditions in neonatal care: use of a manikin of premature baby size. Am J Perinatol 9:239–246

Vanos JK, Rykaczewski K, Middel A, et al (2021) Improved methods for estimating mean radiant temperature in hot and sunny outdoor settings. Int J Biometeorol 65:967–983

Winslow C-E, Gagge Ap, Herrington LP (1939) The influence of air movement upon heat losses from the clothed human body. American Journal of Physiology-Legacy Content 127:505–518

Wissler EH (2018) Human Temperature Control: A quantitative Approach, 1st edn. Springer, Berlin, Germany

Xu J, Psikuta A, Li J, et al (2021a) A numerical investigation of the influence of wind on convective heat transfer from the human body in a ventilated room. Build Environ 188:107427

Xu J, Psikuta A, Li J, et al (2019) Influence of human body geometry, posture and the surrounding environment on body heat loss based on a validated numerical model. Build Environ 166:106340

Xu J, Psikuta A, Li J, et al (2021b) Evaluation of the convective heat transfer coefficient of human body and its effect on the human thermoregulation predictions. Build Environ 196:107778

Yu Y, Liu J, Chauhan K, et al (2020) Experimental study on convective heat transfer coefficients for the human body exposed to turbulent wind conditions. Build Environ 169:106533

Zhang M, Li R, Li J, et al (2021a) A 3D multi-segment thermoregulation model of the hand with realistic anatomy: Development, validation, and parametric analysis. Build Environ 201:107964

Zhang M, Li R, Wu Y, et al (2021b) Numerical study of the convective heat transfer coefficient of the hand and the effect of wind. Build Environ 188:107482

Zhou S, Niu J (2022) Measurement of the convective heat transfer coefficient of the human body in the lift-up design. In: E3S Web of Conferences. EDP Sciences, p 03001

Zou J, Liu J, Niu J, et al (2020) Convective heat loss from computational thermal manikin subject to outdoor wind environments. Build Environ 107469